Defining Sudden Stratospheric Warming in Climate Models: Accounting for Biases in Model Climatologies

JUNSU KIM[a]

Advanced Modeling Infrastructure Team, Numerical Modeling Center, and School of Earth and Environmental Sciences, Seoul National University, Seoul, South Korea

SEOK-WOO SON

School of Earth and Environmental Sciences, Seoul National University, Seoul, South Korea

EDWIN P. GERBER

Courant Institute of Mathematical Sciences, New York University, New York, New York

HYO-SEOK PARK

Korea Institute of Geoscience and Mineral Resources, Daejeon, South Korea

(Manuscript received 20 June 2016, in final form 4 March 2017)

ABSTRACT

A sudden stratospheric warming (SSW) is often defined as zonal-mean zonal wind reversal at 10 hPa and 60°N. This simple definition has been applied not only to the reanalysis data but also to climate model output. In the present study, it is shown that the application of this definition to models can be significantly influenced by model mean biases (i.e., more frequent SSWs appear to occur in models with a weaker climatological polar vortex). To overcome this deficiency, a tendency-based definition is proposed and applied to the multimodel datasets archived for phase 5 of the Coupled Model Intercomparison Project (CMIP5). In this definition, SSW-like events are defined by sufficiently strong vortex deceleration. This approach removes a linear relationship between SSW frequency and intensity of the climatological polar vortex in the CMIP5 models. The models' SSW frequency instead becomes significantly correlated with the climatological upward wave flux at 100 hPa, a measure of interaction between the troposphere and stratosphere. Lower stratospheric wave activity and downward propagation of stratospheric anomalies to the troposphere are also reasonably well captured. However, in both definitions, the high-top models generally exhibit more frequent SSWs than the low-top models. Moreover, a hint of more frequent SSWs in a warm climate is found in both definitions.

1. Introduction

A sudden stratospheric warming (SSW) is an abrupt warming event in the polar stratosphere. It occurs mostly in mid- and late winter (January and February) and almost exclusively in the Northern Hemisphere (Charlton and Polvani 2007). During an event, the polar stratospheric temperature increases by several tens of degrees within a few days and eventually becomes warmer than that of the midlatitudes, reversing the climatological gradient. At the same time, the prevailing westerly wind rapidly decelerates and becomes easterly (Quiroz 1975; Labitzke 1977; Andrews et al. 1987). Based on these observations, an SSW has been often defined as a zonal-mean zonal wind reversal in the polar stratosphere associated with a reversal of the meridional temperature gradient. In this definition, the so-called World Meteorological Organization (WMO) definition, the temperature gradient criterion affects only a very small number of SSWs (Butler et al. 2015). As such, recent studies have often used just the wind reversal criteria and neglected the temperature gradient change. This simple definition, which is referred to as the

[a] Current affiliation: Advanced Modeling Infrastructure Team, Numerical Modeling Center, Seoul, South Korea.

Corresponding author: Seok-Woo Son, seokwooson@snu.ac.kr

DOI: 10.1175/JCLI-D-16-0465.1

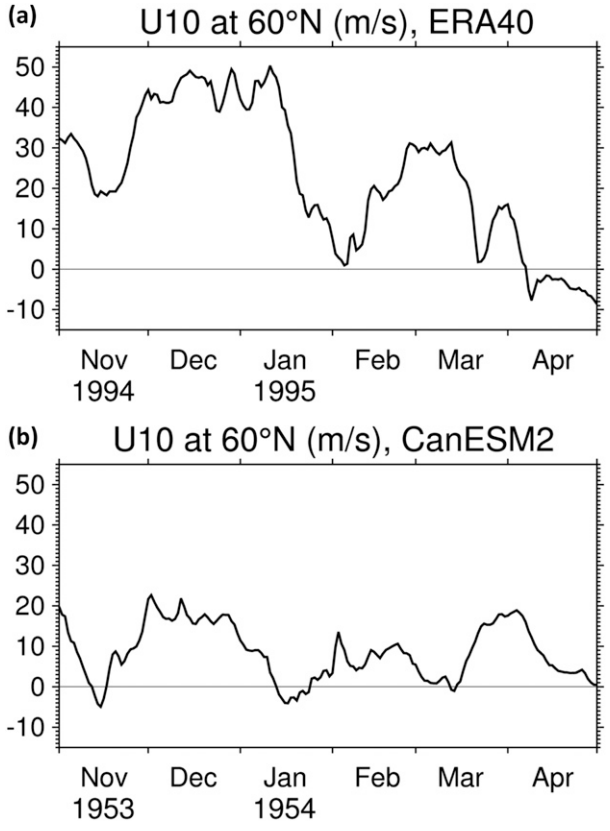

FIG. 1. Zonal-mean zonal winds (m s^{-1}) at 10 hPa and 60°N from representative winters chosen from (a) ERA-40 and (b) the historical integration of CanESM2. The thin line across the x axis denotes the 0 m s^{-1} threshold. Note that these two very different winters were chosen to contrast their qualitative behavior.

wind-reversal definition in the present study, identifies the onset of an SSW as the time at which the 10-hPa zonal-mean zonal wind at 60°N changes its direction from westerly to easterly during the extended winter (e.g., Charlton and Polvani 2007).

It is important to note that the wind-reversal (or WMO) definition is not the only proposed criterion for an SSW. As summarized in Palmeiro et al. (2015), Butler et al. (2015), and Martineau and Son (2015), a number of definitions for SSW have appeared in the literature. These definitions include criteria based on the area-integrated zonal winds, the tendency of the zonal winds, the northern annular mode (NAM) index, an alternative empirical orthogonal function (EOF)-based index, and two-dimensional vortex moment analysis. Palmeiro et al. (2015) documented that the temporal evolution of SSW is not highly sensitive to the details of the definitions, although interannual to decadal variability of SSW is somewhat sensitive (particularly the drought of SSWs in the 1990s; cf. Butler et al. 2015). However, this is not necessarily true for climate models in which the climatology and temporal variability differ from observations. In fact, Palmeiro et al. (2015) reported that the strength of downward coupling between the stratosphere and the troposphere is sensitive to the SSW definition and to the separation of major warming events (i.e., full SSWs) from minor warmings (large perturbations to the polar vortex that do not quite meet the criteria for a full SSW). Definitions that allow more minor warmings to count as full SSWs generally suggest a weaker degree of coupling.

Although the application of the wind-reversal definition to climate model output is straightforward, interpretation of the results is not necessarily obvious. For example, SSWs may occur more frequently in models in which polar vortex variability is anomalously large—that is, models with genuinely more variability. However, SSWs can also appear to occur more frequently in models whose climatological polar vortex is anomalously weak. In this latter case, relatively weak deceleration (i.e., weak wave driving) can result in wind reversal.

As an example, Fig. 1 compares the zonal-mean zonal wind at 10 hPa and 60°N during one winter in reanalysis to another winter selected from a model from phase 5 of the Coupled Model Intercomparison Project (CMIP5). The zonal winds of the 1994/95 winter in reanalysis (Fig. 1a) show the quintessential signature of an SSW: an abrupt deceleration of the zonal wind starting in mid-January. However, the westerly flow never fully reverses; according to the WMO definition, this case is just a minor warming event. In the model (Fig. 1b), the polar vortex is significantly weaker than observed. With this weak background wind, a relatively weak deceleration can cause a wind reversal. Thus, by the WMO criteria, the model exhibits three SSWs between November and March, although the deceleration of the polar vortex in each case is not as pronounced as the minor warming event in the reanalysis data (Fig. 1a). This example suggests that a model could potentially simulate a higher SSW frequency by simply having a weaker vortex, as opposed to exhibiting stronger variability.

This result motivated us to explore the sensitivity of SSWs to biases in model climatologies, which we refer to as a ''model mean bias.'' For multimodel analysis, previous studies have typically used a WMO-like definition (Charlton et al. 2007; Butchart et al. 2011; Charlton-Perez et al. 2008, 2013). Because SSW frequency in the model can be influenced by the model mean bias as described above, it is unclear whether the quantitative assessment of SSW frequency in the literature tells us something about models' variability or, rather, just their climatologies. Although not explored in detail, Butchart

TABLE 1. CMIP5 models used in this study and their classification.

Model name	Center	Vertical levels	Model top	Classification
ACCESS1.0	ACCESS	38	39 km	Low
ACCESS1.3	ACCESS	38	39 km	Low
BCC_CSM1.1	BCC	26	2.917 hPa	Low
BCC_CSM1.1(m)	BCC	26	2.917 hPa	Low
BNU-ESM	College of Global Change and Earth System Science (GCESS), BNU	26	2.194 hPa	Low
CanESM2	CCCma	35	0.5 hPa	Mid
CCSM4	NCAR	27	2.194 hPa	Low
CMCC-CESM	CMCC	39	0.01 hPa	High
CMCC-CM	CMCC	31	10 hPa	Low
CMCC-CMS	CMCC	95	0.01 hPa	High
CNRM-CM5	CNRM	31	10 hPa	Low
CSIRO Mk3.6.0	CSIRO–QCCCE	18	4.5 hPa	Low
FGOALS-g2	LASG/IAP	26	2.194 hPa	Low
GFDL CM3	GFDL	48	0.01 hPa	High
GFDL-ESM2G	GFDL	24	3 hPa	Low
GFDL-ESM2M	GFDL	24	3 hPa	Low
HadGEM2-CC	Met Office Hadley Centre	60	84 km	High
INM-CM4.0	INM	21	10 hPa	Low
IPSL-CM5A-LR	IPSL	39	0.04 hPa	High
IPSL-CM5A-MR	IPSL	39	0.04 hPa	High
IPSL-CM5B-LR	IPSL	39	0.04 hPa	High
MIROC5	Atmosphere and Ocean Research Institute (AORI)/National Institute of Environmental Studies (NIES)/JAMSTEC	40	3 hPa	Low
MIROC-ESM	AORI/NIES/JAMSTEC	80	0.0036 hPa	High
MIROC-ESM-CHEM	AORI/NIES/JAMSTEC	80	0.0036 hPa	High
MPI-ESM-LR	MPI	47	0.01 hPa	High
MPI-ESM-MR	MPI	95	0.01 hPa	High
MRI-CGCM3	MRI	48	0.01 hPa	High
NorESM1-M	Norwegian Climate Centre	26	3.54 hPa	Low

et al. (2011) do attribute a large fraction of the inter-model spread in SSW frequency to the differences in the strength of the polar vortex across models.

In considering model mean bias, this work revisits the assessment of stratospheric variability and SSW frequency in the state-of-the-art climate models archived for the CMIP5. Following previous studies (e.g., Charlton-Perez et al. 2013; Manzini et al. 2014), the models are roughly characterized by grouping them into high-top and low-top models. The low-top models, which have a comparatively poor representation of stratospheric processes, typically underestimate the stratospheric variability and SSW frequency (Charlton-Perez et al. 2013). In this study, it is shown that low-top models underestimate SSW frequency even if a different SSW definition is applied. However, the difference in SSW frequency between the high-top and low-top models becomes smaller when the model mean bias is considered.

This paper is organized as follows. Sections 2 and 3 describe the data used in this study and the definition of SSW. Section 4 explores the climatology, interannual variability, and SSW frequency in the climate change scenario integrations. Section 5 briefly compares the results with scenario integrations in order to examine the potential changes in SSW frequency in a warmer climate.

2. Data

Daily mean zonal-mean zonal wind and geopotential height fields were obtained from the 40-yr European Centre for Medium-Range Weather Forecasts (ECMWF) Re-Analysis (ERA-40; Uppala et al. 2005) for 45 winters of 1957–2002. The results are compared with historical simulations of CMIP5 climate models (listed in Table 1) for the same time period. All models that provide both the historical and representative concentration pathway 8.5 (RCP8.5) simulations are used. Most analyses are performed on the historical runs; RCP8.5 integrations are examined only in section 5 to evaluate possible changes in SSW frequency in a warmer climate. The analysis period of the RCP8.5 runs is 2054–99, allowing a fair comparison with the 45 historical winters. When multiple ensemble members are available, only the first ensemble member (r1i1p1) is

used. An exception is the Community Climate System Model, version 4 (CCSM4), for which the sixth ensemble member (r6i1p1) is used owing to incomplete data in the first ensemble member.

To highlight the model mean bias in the stratosphere, the CMIP5 models are grouped into two subgroups by considering the model top (Charlton-Perez et al. 2013; Manzini et al. 2014). Specifically, models with tops of 1 hPa or higher are classified as high-top models; those with model tops below 1 hPa are classified as low-top models. As described in Table 1, CanESM2 has a model top near 0.5 hPa. It is ambiguous to place this model into either the high-top or low-top category. Following Manzini et al. (2014), this model is therefore classified as a mid-top model.

It is well documented that after an SSW, stratospheric anomalies tend to propagate downward to the troposphere and the surface (Baldwin and Dunkerton 1999; Kodera et al. 2000). Such downward coupling is often evaluated with a so-called dripping paint composite of the NAM index (Baldwin and Dunkerton 2001). In this study, rather than using an EOF-based NAM index, a simple NAM index is used. The NAM index is computed by integrating the geopotential height anomalies from 60°N to the pole at each pressure level (Thompson and Wallace 2000; Gerber et al. 2010). The sign is then flipped to obtain a consistent sign convention of the EOF-based NAM index. All the resulting time series are then normalized by one standard deviation of the variability in ERA-40. This ensures that values of the index for each model represent the same variation of the actual flow as in the reanalysis data.

3. Definition of SSW

In this study, two definitions of SSW are adopted. The wind-reversal definition, requiring a zonal-mean zonal wind reversal at 10 hPa and 60°N, is used as a reference. When an SSW is detected, no subsequent event is allowed within a 20-day interval from the start of the event to avoid a double counting of essentially the same event. The 20-day period is determined in consideration of the thermal damping time scale at 10 hPa. To ensure a focus on midwinter SSWs, final warming events are excluded by adopting the method proposed by Charlton and Polvani (2007).

As discussed earlier, the wind-reversal definition can be impacted by model mean bias. To reduce such dependency, a new definition, which is based on the zonal-mean zonal wind tendency (e.g., Nakagawa and Yamazaki 2006; Martineau and Son 2013), is also applied. Specifically, an SSW-like event is identified when the tendency of zonal-mean zonal wind at 10 hPa and 60°N exceeds $-1.1\,\mathrm{m\,s^{-1}\,day^{-1}}$ over 30 days (i.e., polar vortex deceleration of $-33\,\mathrm{m\,s^{-1}}$ over 30 days). Here, the tendency is computed from 15 days before to after a given day. Note that the reference latitude and pressure level are identical to those used in the wind-reversal definition.

In a tendency-based definition, the two free parameters (i.e., the threshold value of deceleration, $-1.1\,\mathrm{m\,s^{-1}\,day^{-1}}$, and the time window for tendency evaluation, 30 days) were chosen to preserve the same frequency of SSWs in the reanalysis. The 30-day window is inspired by the correlation analysis of Polvani and Waugh (2004). Polvani and Waugh (2004) showed that the upward wave activity entering the stratosphere, integrated over 20 days or longer, leads to a marked weakening of the polar vortex. As discussed in section 4, perturbations to the wave activity associated with SSWs are often maintained for about 30 days. As subsequently described, however, a reasonable adjustment of the analysis window (e.g., 20 or 40 days) does not change the overall results.

Given the 30-day window of analysis, the deceleration threshold, $-1.1\,\mathrm{m\,s^{-1}\,day^{-1}}$, was then set to keep the same frequency of SSWs as found with the WMO definition (6.4 events per decade; Butler et al. 2015; Palmeiro et al. 2015). The sensitivity of SSW frequency to the threshold value will also be discussed below.

It is important to note that the tendency-based definition does not consider a zonal-mean zonal wind reversal. Therefore, the detected SSW includes major SSWs as well as minor warming events in terms of the WMO definition. As such, the number of SSWs and their dynamical evolution in the two definitions are not necessarily the same. Table 2 presents the onset dates of SSWs identified by the wind-reversal and tendency definitions in ERA-40 (see left column for wind-reversal cases). Only 18 events are common to the two definitions. A major difference appears in the early 1990s. Although no SSWs are identified from 1990 to 1997 in the wind-reversal definition, five SSWs are detected in the tendency definition. Overall, the tendency-based SSWs are more evenly distributed in time. This even distribution, with no significant decadal variability, is similar to NAM-based SSW, as shown in Fig. 2 of Butler et al. (2015).

4. Historical runs

a. *Climatology and interannual variability of the polar vortex*

Figure 2a shows a vertical cross section of zonal-mean zonal wind during the Northern Hemisphere winter

TABLE 2. SSW identified from the wind reversal and wind tendency definitions.

Number	Central dates at 60°N	
	Reversal	Tendency
1	31 Jan 1958	30 Jan 1958
2	17 Jan 1960	18 Jan 1960
3	28 Jan 1963	27 Jan 1963
4	16 Dec 1965	
5	23 Feb 1966	27 Feb 1966
6	7 Jan 1968	2 Jan 1968
7	28 Nov 1968	
8	13 Mar 1969	
9	2 Jan 1970	6 Jan 1970
10	18 Jan 1971	15 Jan 1971
11	20 Mar 1971	
12		28 Feb 1972
13	31 Jan 1973	1 Feb 1973
14		28 Feb 1974
15	9 Jan 1977	
16		2 Feb 1978
17		27 Jan 1979
18	22 Feb 1979	27 Feb 1979
19	29 Feb 1980	
20		31 Jan 1981
21	4 Mar 1981	
22	4 Dec 1981	
23		31 Jan 1983
24	24 Feb 1984	19 Feb 1984
25	1 Jan 1985	3 Jan 1985
26	23 Jan 1987	24 Jan 1987
27	8 Dec 1987	10 Dec 1987
28	14 Mar 1988	
29	21 Feb 1989	11 Feb 1989
30		15 Feb 1990
31		4 Feb 1991
32		16 Jan 1992
33		18 Feb 1993
34		27 Jan 1995
35	15 Dec 1998	19 Dec 1998
36	26 Feb 1999	28 Feb 1999
37	20 Mar 2000	
38	11 Feb 2001	9 Feb 2001
39	31 Dec 2001	2 Jan 2002
40	18 Feb 2002	

[December–February (DJF)] from ERA-40. Westerly jets during the boreal winter consist of a tropospheric jet around 30°N and a stratospheric polar vortex around 65°N (Fig. 2a). This structure is well captured by the multimodel mean (MMM) of the high-top models (Fig. 2d). The high-top MMM biases are less than $2\,m\,s^{-1}$ (shaded), which is not significantly different from the ERA-40 data over most regions. In contrast, the low-top MMM show a stronger polar vortex than that in the reanalysis data (Fig. 2g). Their mean biases are larger than $5\,m\,s^{-1}$ at 10 hPa and 40°N, indicating that the polar vortex in the low-top models is biased equatorward. Although a causal relationship is unclear, the wind biases shown in Fig. 2g could partly reflect a lack of SSWs in the low-top models, as compared with reanalyses and the high-top models (Charlton-Perez et al. 2013).

The low-top models also exhibit significantly larger biases in the interannual variability of the extratropical stratosphere than the high-top models (cf. Figs. 2e and 2h). This result, which agrees well with the findings of Charlton-Perez et al. (2013), is to some extent anticipated because the low-top models at best marginally resolve the stratospheric circulation and, in some cases, do not include processes known to be important, such as nonorographic gravity waves. It is interesting to note that both high-top and low-top models underestimate tropical stratospheric variability. This arises from the lack of a quasi-biennial oscillation (QBO) in most models (e.g., Kim et al. 2013). Because the QBO can influence the Northern Hemisphere wintertime stratospheric polar vortex (Holton and Tan 1980; Garfinkel et al. 2012), the lack of QBO activity in the models could adversely affect extratropical stratospheric variability on interannual time scales.

b. *Intraseasonal variability of the polar vortex*

The low-top models again show larger biases in the intraseasonal variability of polar vortex than the high-top models, as quantified by the high-pass-filtered daily standard deviation shown in Figs. 2f and 2i. Here, before computing the daily variability, the seasonal-mean value for each winter was subtracted to remove the interannual variability. These biases in intraseasonal variability are not confined within the stratosphere and extend to the troposphere in high latitudes as well. This could indicate that the poorly represented stratospheric processes in the low-top models may introduce biases in the upper troposphere.

The relationship between the deseasonalized daily zonal-mean zonal wind variability and climatological zonal-mean zonal wind at 10 hPa and 60°N is further illustrated in Fig. 3, where the high-top and low-top models are reasonably well separated into the two clusters. The daily variability in the high-top models is about $12\,m\,s^{-1}$, which is close to the observation of about $13\,m\,s^{-1}$, while that in the low-top models is only about $8\,m\,s^{-1}$. This may indicate less frequent SSWs in the low-top models. In addition, the intermodel spread among the low-top models is larger than that among the high-top models in both climatology and intraseasonal variability. This result confirms that a high model top is helpful for reproducing the stratospheric mean state and temporal variability (Charlton-Perez et al. 2013; Manzini et al. 2014).

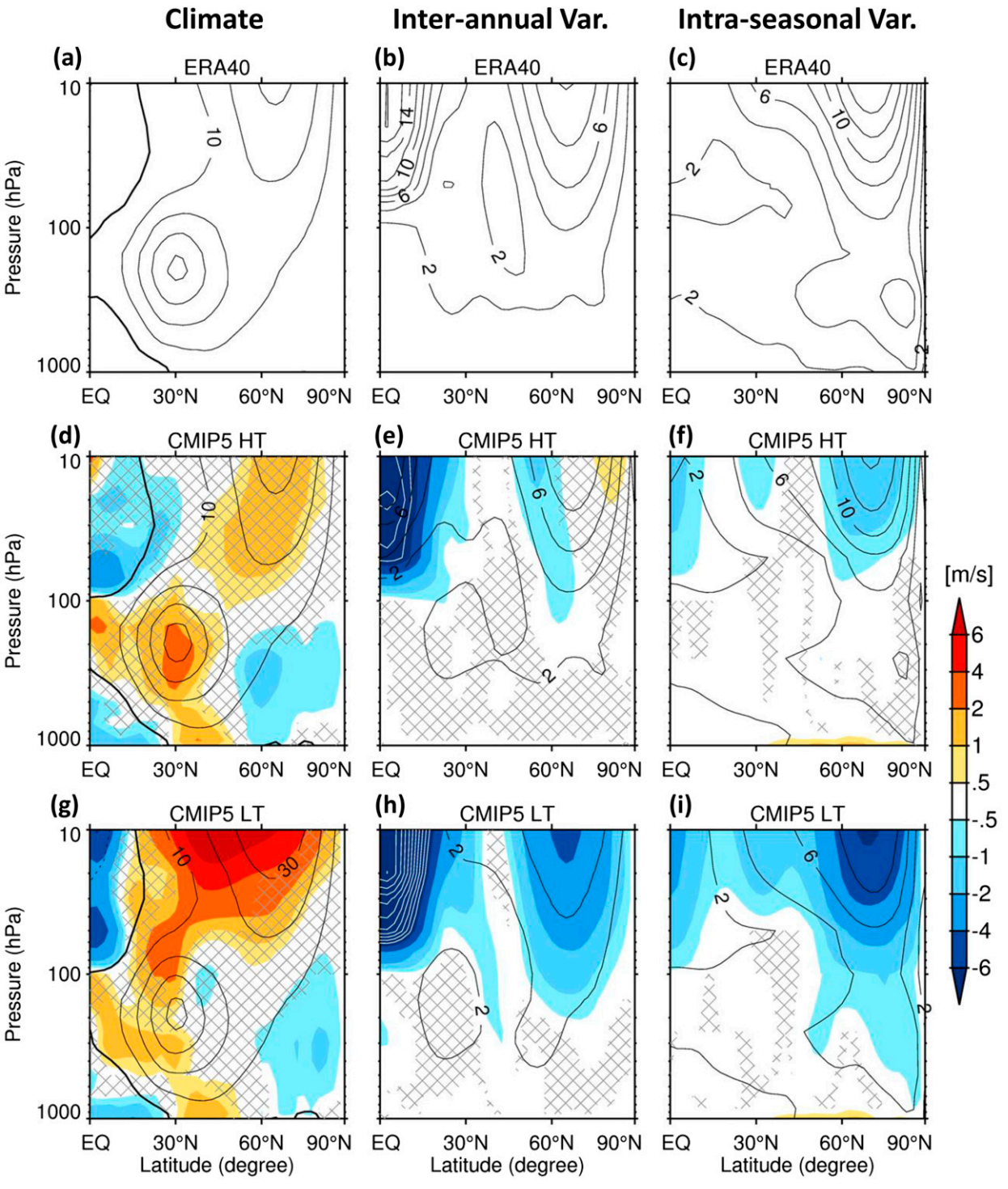

FIG. 2. (a)–(c) Latitude and height cross section of the climatological zonal-mean zonal winds u ($\mathrm{m\,s^{-1}}$) averaged over DJF, and the interannual and intraseasonal variability in ERA-40, respectively; the contour interval in (a) is $10\,\mathrm{m\,s^{-1}}$, and the 0 line is indicated with a thick black line. For the daily variability, the mean value for each winter was subtracted from daily anomalies to remove the impact of the interannual variability. (d)–(f) and (g)–(i) As in (a)–(c), but for high-top and low-top models, respectively. Statistically insignificant (Student's t test; $p > 0.05$) values are hatched, and the bias relative to ERA-40 (model − ERA-40) is shown by the color shading.

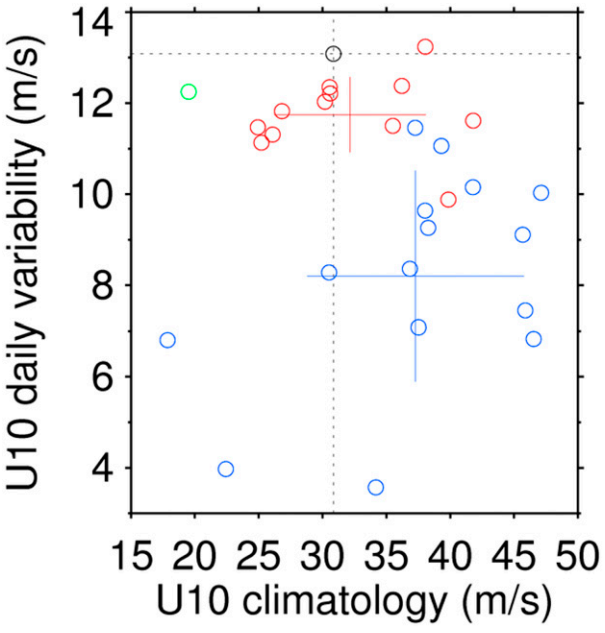

FIG. 3. Scatterplot of the zonal-mean zonal wind climatology at 10 hPa and 60°N and its daily standard deviation from CMIP5 models. Red, green, blue, and black colors indicate high-top, mid-top, and low-top models and ERA-40, respectively. Solid lines indicate plus/minus one standard deviation across the models, centered about their multimodel mean.

c. *SSW statistics*

Following Charlton-Perez et al. (2013), we first evaluate the SSW frequency of ERA-40 with the wind-reversal definition (Fig. 4a). The long-term mean SSW frequency is about 6.4 events per decade, as shown by the horizontal line in Fig. 4a. CMIP5 models typically underestimate this frequency (Charlton-Perez et al. 2013). The SSW frequency in the high-top models varies from 3 to 9 events per decade (red bars), with a MMM frequency of 5.8 events per decade (rightmost red bar). This MMM frequency is reasonably close to the reference frequency. In contrast, the low-top models exhibit only up to 4 events per decade (blue bars in Fig. 4a), with 1.8 events per decade on average (rightmost blue bar). Notably, the intermodel spread in the two groups of models does not overlap: the low-top models are well separated from the high-top models in terms of SSW frequency (see also Fig. 3). This result supports the findings of Charlton-Perez et al. (2013), who analyzed a smaller number of CMIP5 models. Somewhat surprisingly, the mid-top model, CanESM2, shows significantly higher SSW frequency than any other models, with 10.7 events per decade. Such high frequency is associated with a weak background wind in this model, as illustrated in Figs. 1b and 3.

The SSW frequency is also evaluated using the tendency definition (Fig. 4b). By construction, SSW frequency in this definition remains 6.4 events per decade in ERA-40. Although each model exhibits a tendency-based SSW frequency that differs from the wind-reversal definition, the overall frequency of the high-top models is 6.2 events per decade, which is quantitatively similar to the observed frequency. Accounting for the statistical uncertainty range, this frequency is also similar to that derived from the wind-reversal definition: the SSW frequency in the WMO definition is 5.8 events per decade (Fig. 4a), compared to 6.2 events per decades with the tendency-based definition (Fig. 4b). The intermodel spread, however, is only half of that of the wind-reversal definition (cf. Figs. 4a and 4b). This result suggests that the tendency definition is less sensitive to intermodel differences—in particular, model mean biases, as documented below—than the wind-reversal definition.

The low-top models again exhibit fewer SSWs than the high-top models, with an MMM frequency of 3.7 events per decade. This indicates that regardless of the definition, the low-top models tend to underestimate the observed SSW frequency. However, the resulting SSW frequency is larger than that derived from the wind-reversal definition in Fig. 4a (i.e., 3.7 vs 1.8 events per decade). Hence, the difference in SSW frequency between the high-top and low-top models becomes smaller when the tendency definition is used. In fact, the intermodel spread of SSW frequency in the low-top models now overlaps that in the high-top models (Fig. 4b). This result indicates that the frequency of extreme stratospheric events may be less sensitive to the model top than that previously reported (e.g., Charlton-Perez et al. 2013). This is particularly true if the two models with extremely rare SSWs (i.e., CSIRO Mk3.6.0 and INM-CM4.0) are excluded from the low-top MMM.

The only mid-top model, CanESM2, shows a significant reduction in SSW frequency from the wind-reversal definition to the tendency definition, as indicated by the green bars in Figs. 4a and 4b. When the tendency definition is used, SSW frequency becomes close to the observed frequency. The CanEMS2, which is a clear outlier in terms of the wind-reversal SSWs (not belonging to either high-top or low-top models) is no longer an outlier.

The above results are all based on intercomparison of high-top and low-top models. However, even in each group, individual models are very different in many aspects, such as dynamic core, physics, resolution, and ocean models. Therefore, direct comparison of these models may not be straightforward. In this regard, comparison of two different experiments from the same modeling institutes might be insightful.

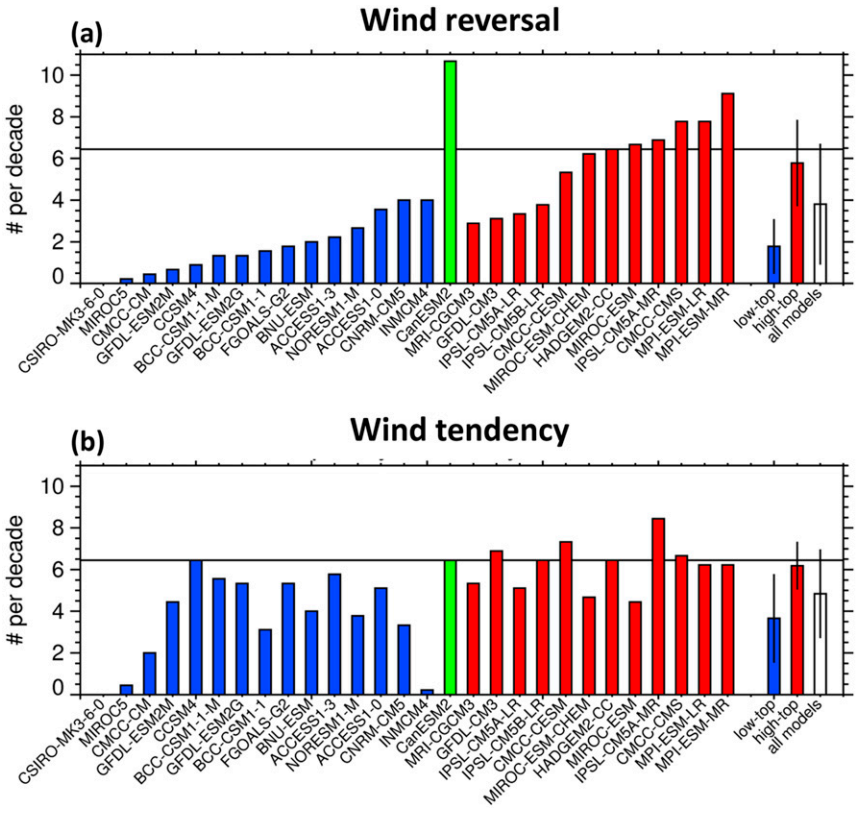

FIG. 4. SSW frequency derived from (a) the wind-reversal definition and (b) the wind tendency definition. Low-top, mid-top, and high-top models are colored blue, green, and red, respectively. The SSW frequency in ERA-40 is indicated by the black horizontal line. Multimodel mean frequency and intermodel spread (one standard deviation) are shown at the right of each panel.

As indicated in Table 1, the Centro Euro-Mediterraneo per I Cambiamenti Climatici (CMCC) provides two experiments (i.e., CMCC-CM and CMCC-CMS). The former is a low-top version, whereas the latter is a high-top version of the model. Figure 4b shows that CMCC-CMS simulates realistic SSW frequency and significantly more frequent SSW than CMCC-CM, which is consistent with the MMM comparison. A pair of experiments from L'Institut Pierre-Simon Laplace Coupled Model, version 5A (IPSL-CM5A)—specifically, the IPSL-CM5A low resolution (LR) and IPSL-CM5A mid resolution (MR) models, which differ in horizontal resolution—suggests that a model with higher horizontal resolution will simulate more frequent SSWs. However, the MPI-ESM-LR and MPI-ESM-MR, which have different vertical resolutions but the same model top, show a similar SSW frequency. A comparison of the Model for Interdisciplinary Research on Climate, Earth System Model (MIROC-ESM), and that coupled with stratospheric chemistry (MIROC-ESM-CHEM) also shows no significant difference. Altogether, these results may suggest that SSW frequency is more sensitive to the model top and horizontal resolution than to vertical resolution and interactive chemistry (Scott et al. 2004). However, to confirm this speculation, additional modeling studies with systematic varying of model configurations are needed.

To highlight the dependency of SSW frequency on the model mean bias, Fig. 5a illustrates the relationship between DJF-mean zonal-mean zonal wind at 10 hPa and 60°N and SSW frequency derived from the wind-reversal definition. The high-top, mid-top, and low-top models are indicated in red, green, and blue, respectively, whereas ERA-40 is shown by a black dot. A strong negative correlation is evident with a correlation coefficient of −0.63, which is statistically significant at the 95% confidence level. This clearly indicates that SSW occurs less frequently as the background wind becomes stronger (or, alternatively, fewer SSWs lead to a stronger vortex). Such negative correlation is somewhat weak in the low-top models owing to a few outliers that have almost no SSWs. Without these

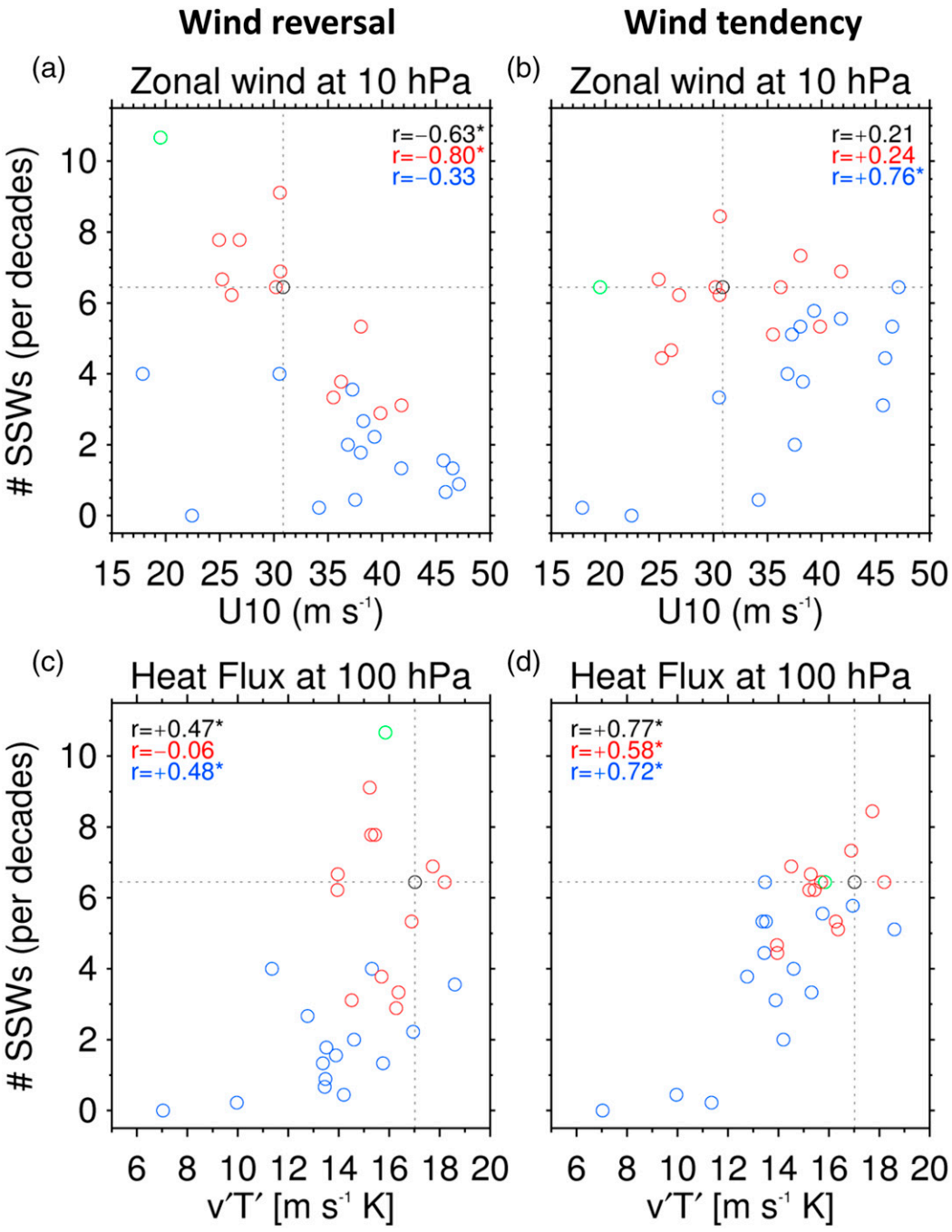

FIG. 5. (top) Scatterplots of the climatological zonal-mean zonal wind at 10 hPa and 60°N and SSW frequency for (left) the wind-reversal definition and (right) the wind tendency definition. (bottom) As in (top), but for the climatological eddy heat flux at 100 hPa averaged over 45°–75°N. Low-top, mid-top, and high-top models are colored blue, green, and red, respectively. Black-dotted lines indicate the reference values in ERA-40. The numbers shown in each panel denote the correlation coefficients for all (black), high-top (red), and low-top (blue) models. Statistically significant correlation at the 95% confidence level is indicated by an asterisk.

outliers (i.e., CSIRO Mk3.6.0 and MIROC5), the negative correlation becomes statistically significant.

Figure 5a also shows that the high-top models are well separated from the low-top models. Except for two models, most low-top models show a stronger polar vortex than ERA-40. This strong polar vortex does not allow a wind reversal unless stratospheric wave driving is sufficiently strong or may inhibit resonance in the case

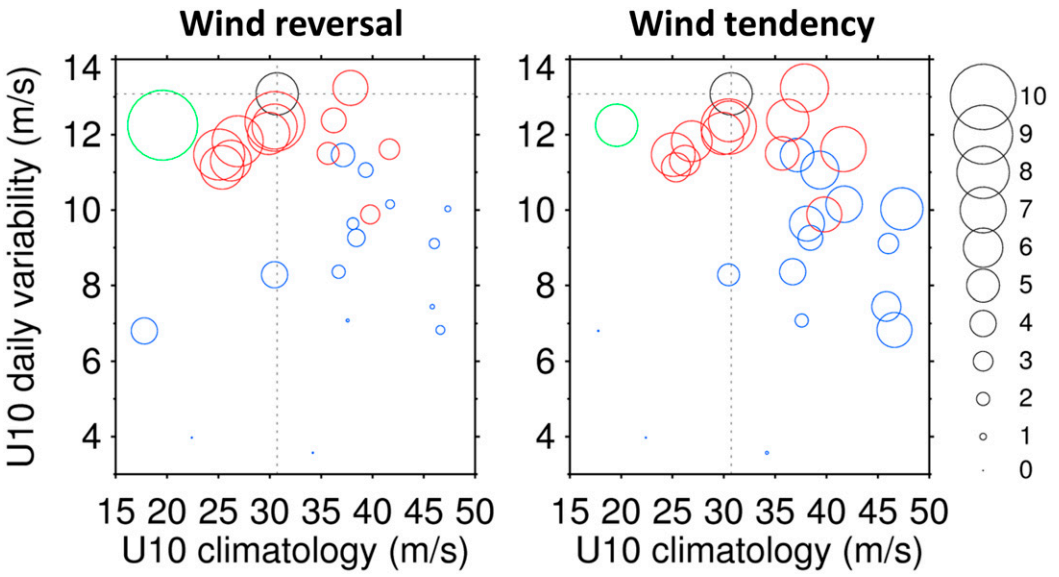

FIG. 6. As in Fig. 3, but for SSW frequency based on (left) the wind reversal definition and (right) the wind tendency definition. The circle size indicates the SSW frequency per decade. Low-top, mid-top, and high-top models are colored blue, green, and red, respectively.

of a vortex split event, which depends less on the wave driving (Esler and Scott 2005). This result confirms that the difference between the high-top and low-top models shown in Fig. 4a is caused partly by the model mean biases. Another factor that may explain the less frequent SSW in the low-top models is the relatively weak wave driving. As shown in Fig. 5c, the low-top models exhibit somewhat weaker wave activity than the high-top models. Here, wave activity is quantified by the time mean, zonal-mean eddy heat flux at 100 hPa integrated over 45°–75°N (Polvani and Waugh 2004).

Figure 5 (right) is identical to Fig. 5 (left) except for the tendency definition. The linear relationship evident in Fig. 5a essentially disappears in Fig. 5b. Note that although the low-top models show a statistically significant correlation, the correlation coefficient is positive, which is largely attributed to the two outliers at the bottom left-hand corner. This result suggests that the tendency definition is almost independent of model mean biases. More importantly, the tendency definition is strongly correlated with the wave activity at 100 hPa (Fig. 5d): more frequent SSW occurs when the wave activity in the lower stratosphere is stronger. This result may indicate that the tendency definition is more dynamically relevant than the wind-reversal definition. Here it should be noted that most models underestimate wave activity in the lower stratosphere. This is consistent with the fact that most models underestimate the SSW frequency regardless of the model top (Fig. 4b).

The relationships between SSW frequency, daily zonal-mean zonal wind variability, and DJF-mean zonal-mean zonal wind at 10 hPa and 60°N are summarized in Fig. 6, which combines the essential results of Figs. 3, 5a, and 5b. The CMIP5 models generally have realistic time-mean polar vortices but too little variability (e.g., climatology of 25–35 m s^{-1} in Fig. 6). For both the wind-reversal and tendency definitions, the CMIP5 models exhibit less frequent SSWs and weaker intraseasonal variability in comparison to ERA-40. This is particularly true for the low-top models. However, unlike the tendency-based SSW frequency, the wind-reversal SSW frequency exhibits a strong dependence on the climatological wind, with less frequent SSWs associated with strong background wind (smaller circles for climatological wind stronger than 35 m s^{-1}). This impact of model mean bias is effectively removed in the tendency definition.

We next explore the sensitivity of subseasonal distribution of SSW frequency to the SSW definition. Previous studies have reported that climate models have trouble producing the correct monthly distribution of SSW frequency under the wind-reversal definition (Schmidt et al. 2013; Charlton et al. 2007). Figure 7 shows the monthly distribution of SSWs for the wind-reversal and tendency definitions. SSWs from ERA-40 are shown in black, and those from high-top and low-top models are shown in red and blue, respectively. With the wind-reversal definition (Fig. 7a), SSWs in ERA-40 occur throughout the extended winter season but peak in midwinter (January). As noted by earlier studies, the distribution of wind-reversal events is too evenly spread across the extended winter in high-top models and heavily biased toward late winter in low-top models.

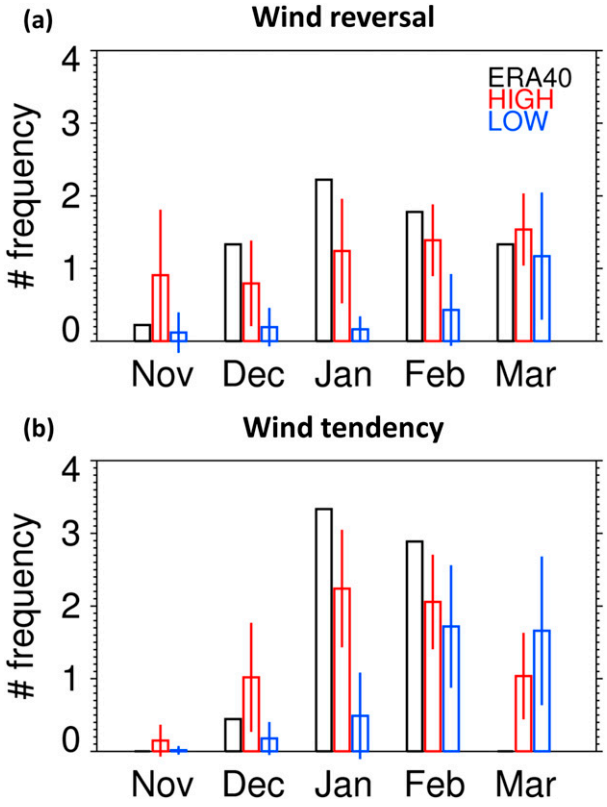

FIG. 7. Distribution of stratospheric warmings by month in ERA-40 (black), high-top (red), and low-top models (blue) derived from (a) the wind-reversal definition and (b) the wind tendency definition. Vertical lines at high-top and low-top models indicate the plus/minus one standard deviation of SSW frequency from the mean of each model.

The tendency definition tends to concentrate SSWs in January and February (Fig. 7b). We believe that this stems from the fact that a large absolute deceleration of the vortex in part depends upon a strong initial vortex. Once the winds reverse, Rossby wave propagation is inhibited, limiting any further wave breaking that would be needed to drive the winds more strongly negative. Hence, events are favored by the strong climatological wind in midwinter. Note that the final warmings are naturally excluded in the tendency definition, given the weakness of the polar vortex in late winter. This focusing of events in the midwinter is captured in high-top models, although the distribution is still too flat, with too many events in November, December, and March and too few in January and February. The low-top models again fail to capture the subseasonal distribution of SSW events, with events concentrated at the very end of winter.

d. SSW dynamics

The SSWs identified by the two definitions may exhibit different dynamical evolution. For example, linear wave dynamics suggest that vertical propagation of planetary-scale waves, which drive SSW, can be restricted if the zonal wind in the stratosphere becomes easterly. However, this may not be the case in the tendency-based SSW events because easterly wind reversal is not guaranteed and minor warming events (in terms of the WMO definition) are included. To address this issue, we investigate the evolution of wave activity over the course of SSW events characterized by both definitions. Figure 8 presents composites of the temporal evolution of zonal-mean eddy heat flux at 100 hPa integrated over 45°–75°N. The heat flux increases before the onset of an SSW and then rapidly decreases afterward. Although the evolution of wave activity is qualitatively similar in the two definitions, the tendency definition shows a somewhat slower decay, as shown by the black lines in Fig. 8. In this respect, the tendency-based SSW events are less "sudden." Furthermore, a small amount of planetary-scale waves still propagates into the stratosphere even after the event onset because not all events accompany a wind reversal.

The wind-reversal SSWs are associated with slightly stronger and more concentrated wave forcing than that of the tendency-based SSWs. However, the time-integrated wave activity over 30 days before the onset of SSW is comparable in the two definitions, indicating similar net wave driving. Figure 8 also shows that the wave activity in the high-top models is somewhat stronger than that in the low-top models from lag −20 to 0 days. Consistent with this result, the intensity of SSWs (in terms of zonal wind deceleration) is somewhat stronger in the high-top models than that in the low-top models (not shown). This result suggests that improved vertical resolution and a higher model top is helpful in simulating more realistic SSWs.

As discussed previously, SSWs have received much attention in recent decades because of their influence on the tropospheric circulation and surface climate (Baldwin and Dunkerton 2001). By comparing a subset of CMIP5 models, Charlton-Perez et al. (2013) reported that high-top models tend to have more persistent anomalies than low-top models in the troposphere. In Fig. 9, a similar comparison is made in terms of NAM-index anomalies for the two SSW definitions. For ERA-40, the tendency-based SSWs exhibit a stronger phase change than the wind-reversal SSWs in NAM anomalies in both the lower stratosphere and the troposphere (Figs. 9a,b), but an overall weaker (less negative) tropospheric NAM response follows the event. Such a difference is also evident in the analysis of individual models. This result implies that the wind-reversal SSWs are somewhat deeper than the tendency-based SSWs. The exact reason is not clear. However, it is consistent with stronger and more abrupt wave flux changes in the wind-reversal events (Fig. 8).

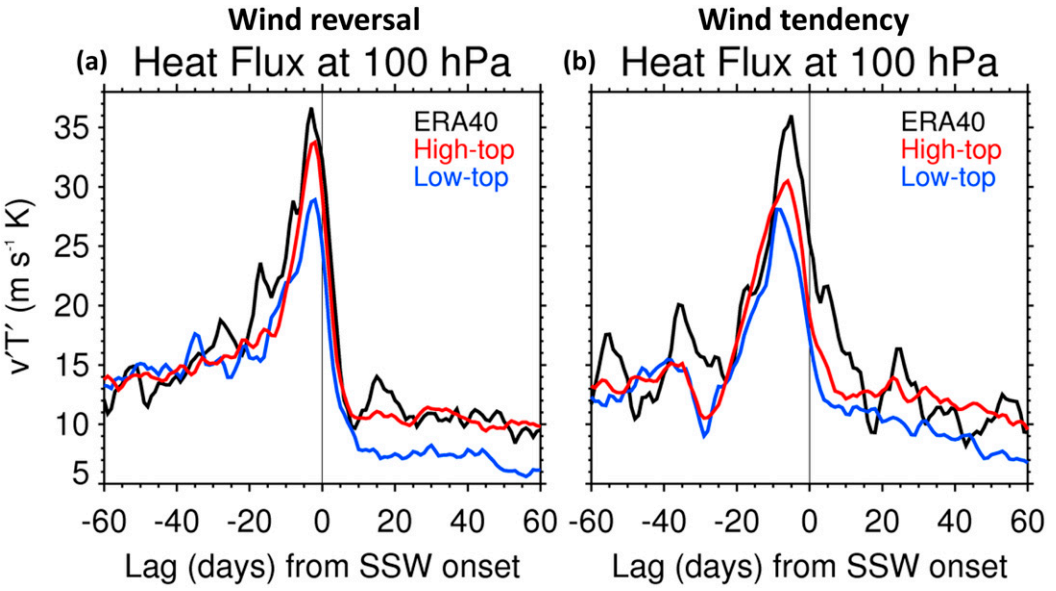

FIG. 8. Multimodel mean composite time series of zonal-mean eddy heat flux at 100 hPa averaged over 45°–75°N during SSWs detected by (a) the wind reversal definition and (b) the wind tendency definition. Lag zero indicates the onset of the SSW. Low-top and high-top models are denoted by blue and red colors, respectively. The reference time series, derived from ERA-40, is shown in black.

A rather weak tropospheric response to tendency based SSWs may result from the inclusion of minor warmings (in terms of the WMO definition) and the spread of onset dates. In the tendency definition, zonal-wind tendency is computed with a 30-day time window and the onset date is simply set to be the central date. This central day is not necessarily the day of maximum vortex deceleration. This mismatch could cause weaker SSWs and weaker downward coupling. However, the resulting downward coupling is still within an uncertainty range of various SSW definitions as shown in Fig. 6 of Palmeiro et al. (2015).

It is important to note in Fig. 9 that SSW-induced NAM-index anomalies in the lower stratosphere tend to persist longer in the high-top models than in the low-top models. For example, with the wind-reversal definition, 100-hPa anomalies exceeding (more negative than) −1 extend about 40 days in high-top models but only 30 days in low-top models. For the tendency-based definition, an anomaly exceeding −0.5 persists for about 40 days in the high-top models, as compared to 35 days in the low-top models. Similarly, the tropospheric anomalies are stronger and persist slightly longer in the high-top models than in the low-top models with both definitions. This result suggests that the time scale of SSWs and their downward coupling are potentially sensitive to the model top.

e. *Sensitivity test*

Both the WMO wind-reversal and tendency-based definitions focus on the zonal-mean zonal wind at a fixed latitude (60°N). This latitude corresponds to the vortex boundary in the reanalysis data (Butler et al. 2015). However, the same may not be true in models. In fact, as shown in Fig. 2, the latitudinal structure of the polar vortex in the model differs from that in the reanalysis data, and 60°N is not the vortex boundary in all models. This is particularly true for the low-top models (Fig. 2g). To test this possibility, all analyses are repeated by replacing the fixed reference latitude with the model-dependent reference latitudes. The latitude of the maximum zonal-mean zonal wind at 10 hPa in long-term climatology is chosen for each model, and the SSW frequency is reevaluated. This modification results in an increased SSW frequency of about half an event per decade in both the high-top and low-top models (not shown). However, the overall conclusion of more frequent SSWs in high-top models than those in low-top models does not change.

We also tested the sensitivity of the tendency-based SSWs to the threshold value of deceleration and the time window of tendency evaluation. Figure 10 (top) presents the SSW frequency calculated from ERA-40 as a reference. As anticipated, the SSW frequency generally increases as the threshold value decreases (i.e., SSW is more frequent for a weaker threshold value). The SSW frequency also decreases with an increase in the time window. Notably, the SSW frequency in the high-top models is comparable to that in ERA-40 if the observed SSW frequency of 6–8 events per decade is selected as a reference (near-zero line in Fig. 10c) but

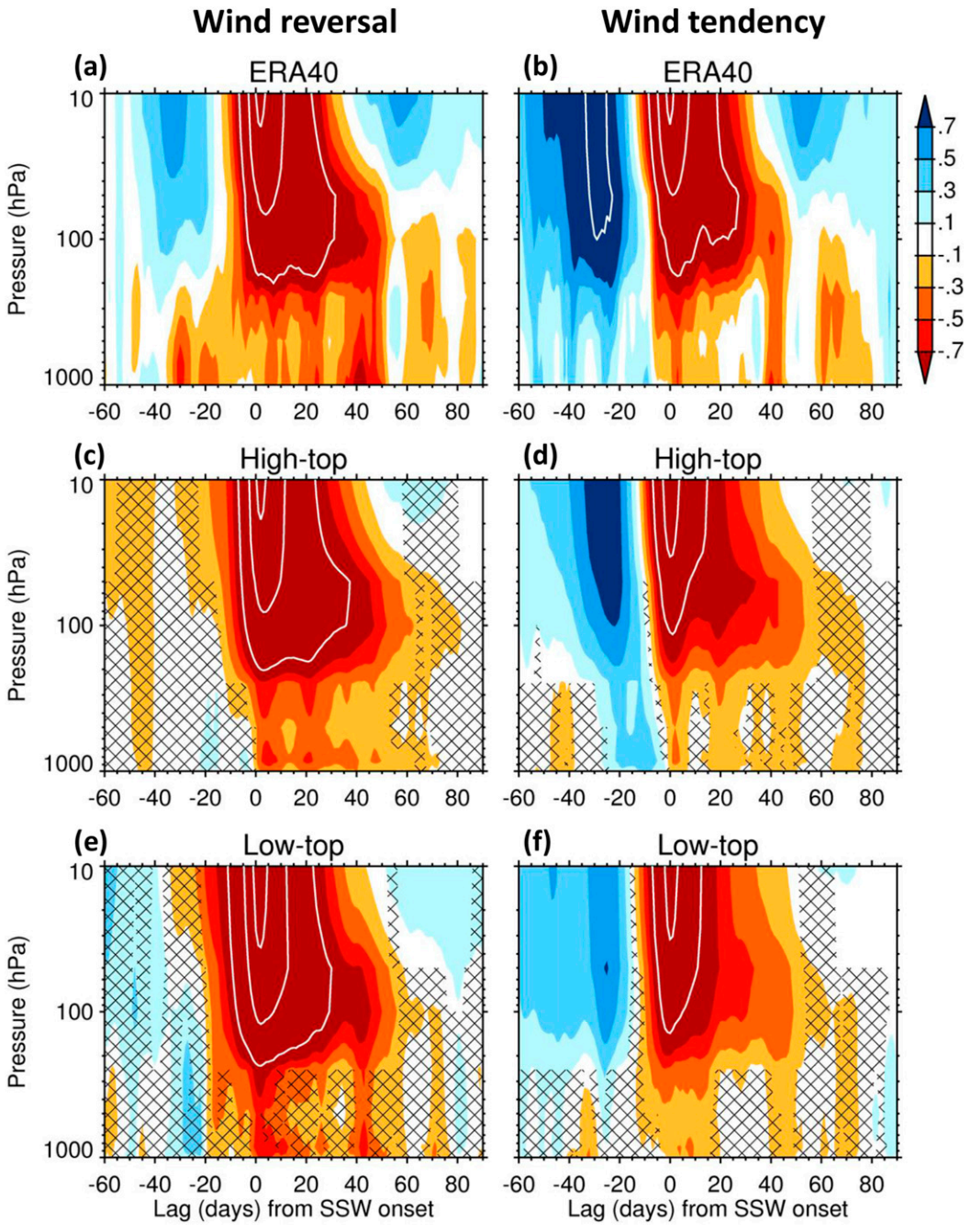

FIG. 9. Time–height development of the NAM index during SSW events, as detected by (left) the wind-reversal definition and (right) the wind tendency definition for (a),(b) ERA-40; (c),(d) high-top; and (e),(f) low-top models. The NAM index is based on polar-cap-averaged geopotential height (>60°N). Contour intervals of one standard deviation are indicated by the white lines. Hatching shows insignificant values (95%) when the multimodel spread is considered.

would be biased high (low) if stricter (weaker) criteria are applied. The low-top models, however, exhibit significantly fewer SSWs (Fig. 10d) under all conditions, such that the underestimation is not highly sensitive to the parameters used in the tendency definition. This indicates that the SSW frequency difference between the two groups of models (Fig. 10b) is a very robust result.

Last, Fig. 11 illustrates the relationship between the SSW frequency and the climatological vortex (as in

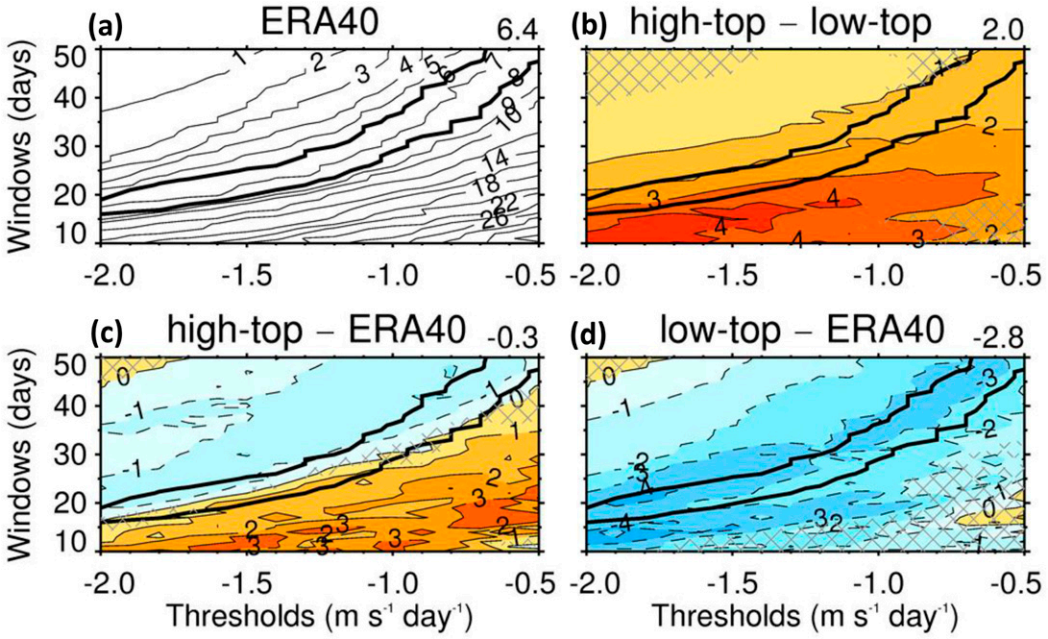

FIG. 10. (a) SSW frequency as a function of the threshold value of the zonal-mean zonal wind tendency at 10 hPa and 60°N and the evaluated time window, for ERA-40. The difference is shown between (b) the high-top and low-top models and between ERA-40 and the (c) high-top and (d) low-top models. Values statistically insignificant at the 95% confidence level are hatched. Two low-top models were excluded because they simulate SSWs extremely rarely. The SSW frequency of six to eight events per decade from ERA-40 is shown by with thick black lines in each panel. The numbers at the upper-right corner in each panel indicates SSW frequency or its difference from ERA-40 when the standard $-1.1\,\mathrm{m\,s^{-1}\,day^{-1}}$ threshold and 30-day time window are used.

Figs. 5a,b) but based on winds at 65° and 70°N. The overall results are essentially the same as the analysis at 60°N (cf. Figs. 5a, 5b, and 11). A strong negative correlation in the wind-reversal definition (Figs. 11a,c) disappears in the tendency definition (Figs. 11b,d). This result suggests that the results presented in the previous section are not sensitive to the choice of reference latitude.

5. SSWs in future climate projections

We now compare the SSW frequency in the recent past with that of the late twenty-first century in a high carbon future. Figure 12 illustrates the projected changes in SSW frequency under the RCP8.5 scenario. The wind-reversal definition suggests slightly more frequent SSW in a warmer climate (Fig. 12a), which agrees well with the results of Charlton-Perez et al. (2008). The high-top models generally show a more positive trend than the low-top models: 8 out of 12 high-top models show an increasing trend (Fig. 12c). However, the low-top models do not show a clear trend. If CSIRO Mk3.6.0, which fails to simulate any SSWs, is excluded, the number of the models with an increasing versus decreasing trend are the same.

McLandress and Shepherd (2009) suggested that the increasing trend of SSW frequency in warm climate may be partly attributed to changes in background wind rather than in wave activity and actual variability of the vortex. In response to increasing greenhouse gas concentration, the polar vortex tends to weaken (e.g., McLandress and Shepherd 2009; Manzini et al. 2014; Mitchell et al. 2012; Ayarzagüena et al. 2013). If the background wind becomes weaker in a warmer climate, the chances of a wind reversal may increase, resulting in more frequent SSWs (McLandress and Shepherd 2009). By using a relative definition that is not sensitive to the mean flow change, McLandress and Shepherd (2009) in fact showed that SSW frequency does not change much in their model simulation.

This idea is evaluated with a tendency definition (Fig. 12b). It is found that, in both the high-top and low-top models, SSW frequency is projected to slightly increase in the future. Although the absolute change is not statistically significant, 21 of 27 CMIP5 models show an increasing trend (Fig. 12d). Such behavior is also evident upon separate examination of the high-top and low-top models, with 9 of 12 high-top and 11 of 14 low-top models showing increasing trends. This result suggests that stratospheric extreme events may indeed increase

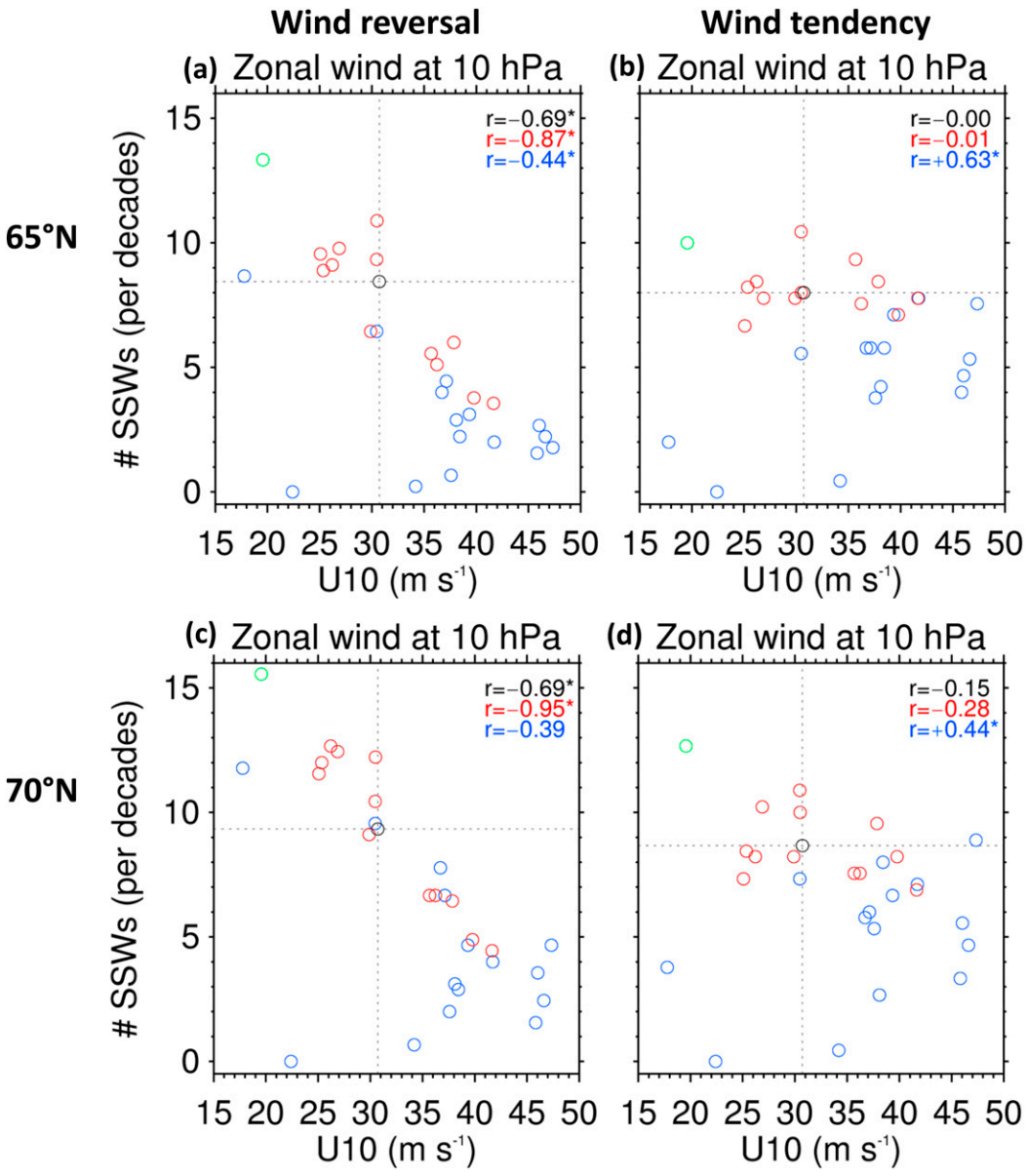

FIG. 11. (a),(b) Scatterplots of climatological zonal-mean zonal wind at 10 hPa and 65°N, and SSW frequency for (left) the wind-reversal definition and (right) the wind tendency definition. (c),(d) As in (a),(b), but for zonal wind at 70°N. Low-top, mid-top, and high-top models are colored with blue, green, and red, respectively. Black-dotted lines indicate the reference values in ERA-40. Numbers shown in each panel denote the correlation coefficients for all (black), high-top (red), and low-top models (blue). Statistically significant correlation coefficients at the 95% confidence level are indicated by asterisk.

in the future climate. To identify the dynamical mechanism(s), further analyses are needed.

6. Summary and discussion

Our analysis suggests that the frequency of SSWs identified with the WMO definition (i.e., a wind reversal at 10 hPa and 60°N) is very sensitive to model mean biases (McLandress and Shepherd 2009). If the climatological polar vortex of a model is stronger (weaker) than in observations, it tends to simulate less (more) frequent SSWs. A fairly linear relationship between SSW frequency and vortex strength is found in the CMIP5 models regardless of the reference latitude (e.g., 60°, 65°, and 70°N). This suggests that previous multimodel studies of wind-reversal SSWs are likely

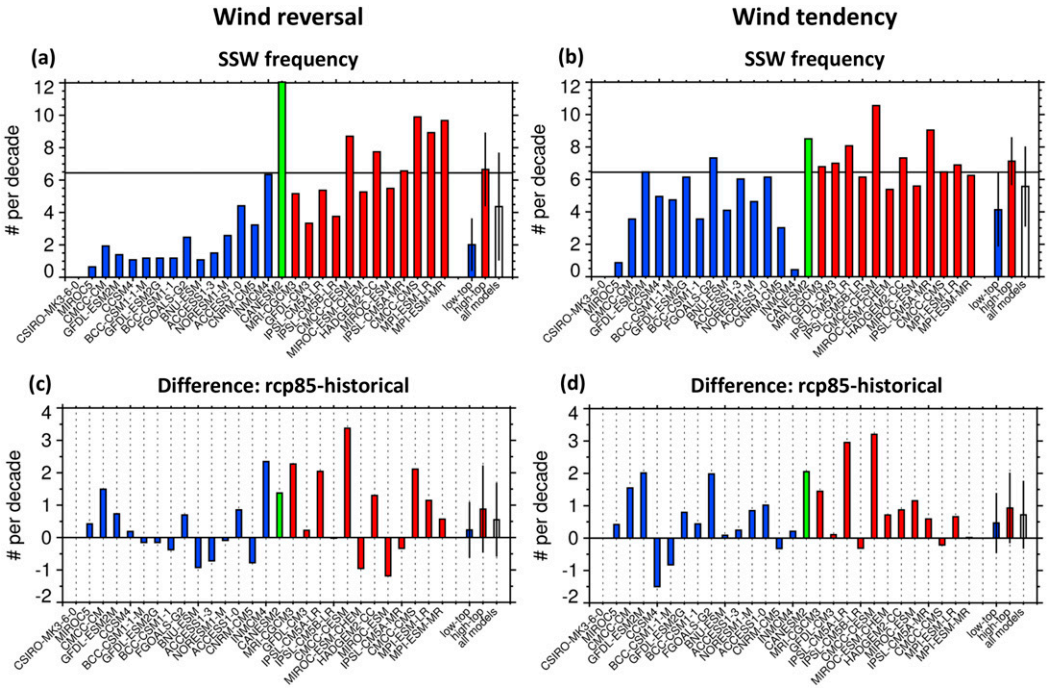

FIG. 12. (a),(b) As in Fig. 4, but for years 2054–99 in the RCP8.5 integrations. (c),(d) Difference in SSW frequency between RCP8.5 and historical runs.

influenced by model mean biases and long-term mean flow changes (Fig. 2).

An alternative definition of SSW, aiming to make it independent of model mean biases, was proposed. This definition detects SSWs by examining the zonal-mean zonal wind tendency at 10 hPa and 60°N; with this definition, the linear relationship between SSW frequency and the intensity of climatological polar vortex essentially disappears. Final warming events are also naturally filtered out. More importantly, SSW frequency becomes highly correlated with upward-propagating wave activity at 100 hPa. This result indicates that the tendency definition is more dynamically connected to stratospheric variability than the wind-reversal definition. This is anticipated because the zonal-mean zonal wind tendency is directly related to eddy heat (and momentum flux) divergence in the transformed Eulerian mean framework.

The tendency definition results in more frequent SSWs than the wind-reversal definition in the climate models, even though it was constructed to have no impact on the frequency in reanalysis. This is particularly true for the low-top models. This indicates that the significant difference in SSW frequency between the low-top and high-top models reported in previous studies (e.g., Charlton-Perez et al. 2013) can be attributed, at least in part, to model mean biases rather than differences in wave driving. However, with both definitions, the high-top models show more realistic SSW statistics than the low-top models. In particular, the low-top models significantly underestimate SSW frequency, which is consistent with the relatively weak amount of wave driving observed in their lower stratospheres, and they fail to simulate the seasonal distribution of SSW events. This result indicates that a high model top and more accurate stratospheric representation are necessary for simulating realistic SSW statistics. It is also found that, with both definitions, the SSW frequency is projected to increase in a warm climate. These results are qualitatively consistent with those in previous studies (e.g., Charlton-Perez et al. 2008, 2013).

The SSWs detected by the different definitions have different dynamical and physical properties (Martineau and Son 2015). The tendency-based SSWs show quantitatively different temporal evolution compared to wind-reversal SSWs. The former is associated with less focused and slightly weaker wave activity than the latter. This difference leads to slightly weaker persistence of stratospheric anomalies and weaker downward coupling to the troposphere for tendency-based events. However, such differences are still within the uncertainty of various SSW definitions (Palmeiro et al. 2015).

It should be emphasized that the development of a new SSW definition was not the primary intent in this

study. Our main objectives were to reexamine the SSW frequency in climate models in light of biases in their climatological polar vortices and to test the robustness of previous studies to the exact details of the SSW definition. Certainly, other approaches could be developed to define stratospheric extreme events that are insensitive to model mean biases (e.g., Palmeiro et al. 2015; Butler et al. 2015; Martineau and Son 2015). Since many different definitions of SSWs have been used in the literature, further discussion on their weaknesses and strengths would be valuable (Butler et al. 2015).

Acknowledgments. The authors thank all of the reviewers for their helpful comments. The authors thank Dr. Gwangyong Choi for offering helpful discussion. This work was funded by the Korea Meteorological Administration Research and Development Program under Grant KMIPA 2015-2094 and the U.S. National Science Foundation, through Grant AGS-1546585.

REFERENCES

Andrews, D. G., J. R. Holton, and C. B. Leovy, 1987: *Middle Atmosphere Dynamics*. Academic Press, 489 pp.

Ayarzagüena, B., U. Langematz, S. Meul, S. Oberländer, J. Abalichin, and A. Kubin, 2013: The role of climate change and ozone recovery for the future timing of major stratospheric warmings. *Geophys. Res. Lett.*, **40**, 2460–2465, doi:10.1002/grl.50477.

Baldwin, M. P., and T. J. Dunkerton, 1999: Propagation of the Arctic Oscillation from the stratosphere to the troposphere. *J. Geophys. Res.*, **104**, 30 937–30 946, doi:10.1029/1999JD900445.

——, and ——, 2001: Stratospheric harbingers of anomalous weather regimes. *Science*, **294**, 581–584, doi:10.1126/science.1063315.

Butchart, N., and Coauthors, 2011: Multimodel climate and variability of the stratosphere. *J. Geophys. Res.*, **116**, D05102, doi:10.1029/2010JD014995.

Butler, A. H., D. J. Seidel, S. C. Hardiman, N. Butchart, T. Birner, and A. Match, 2015: Defining sudden stratospheric warmings. *Bull. Amer. Meteor. Soc.*, **96**, 1913–1928, doi:10.1175/BAMS-D-13-00173.1.

Charlton, A. J., and L. M. Polvani, 2007: A new look at stratospheric sudden warmings. Part I: Climatology and modeling benchmarks. *J. Climate*, **20**, 449–469, doi:10.1175/JCLI3996.1.

——, and Coauthors, 2007: A new look at stratospheric sudden warmings. Part II: Evaluation of numerical model simulations. *J. Climate*, **20**, 470–488, doi:10.1175/JCLI3994.1.

Charlton-Perez, A. J., L. M. Polvani, J. Austin, and F. Li, 2008: The frequency and dynamics of stratospheric sudden warmings in the 21st century. *J. Geophys. Res.*, **113**, D16116, doi:10.1029/2007JD009571.

——, and Coauthors, 2013: On the lack of stratospheric dynamical variability in low-top versions of the CMIP5 models. *J. Geophys. Res. Atmos.*, **118**, 2494–2505, doi:10.1002/jgrd.50125.

Esler, J. G., and R. K. Scott, 2005: Excitation of transient Rossby waves on the stratospheric polar vortex and the barotropic sudden warming. *J. Atmos. Sci.*, **62**, 3661–3682, doi:10.1175/JAS3557.1.

Garfinkel, C. I., T. A. Shaw, D. L. Hartmann, and D. W. Waugh, 2012: Does the Holton–Tan mechanism explain how the quasi-biennial oscillation modulates the Arctic polar vortex? *J. Atmos. Sci.*, **69**, 1713–1733, doi:10.1175/JAS-D-11-0209.1.

Gerber, E. P., and Coauthors, 2010: Stratosphere–troposphere coupling and annular mode variability in chemistry–climate models. *J. Geophys. Res.*, **115**, D00M06, doi:10.1029/2009JD013770.

Holton, J. R., and H.-C. Tan, 1980: The influence of the equatorial quasi-biennial oscillation on the global circulation at 50 mb. *J. Atmos. Sci.*, **37**, 2200–2208, doi:10.1175/1520-0469(1980)037<2200:TIOTEQ>2.0.CO;2.

Kim, J., K. M. Grise, and S.-W. Son, 2013: Thermal characteristics of the cold-point tropopause region in CMIP5 models. *J. Geophys. Res. Atmos.*, **118**, 8827–8841, doi:10.1002/jgrd.50649.

Kodera, K., Y. Kuroda, and S. Pawson, 2000: Stratospheric sudden warmings and slowly propagating zonal-mean zonal wind anomalies. *J. Geophys. Res.*, **105**, 12 351–12 359, doi:10.1029/2000JD900095.

Labitzke, K., 1977: Interannual variability of the winter stratosphere in the Northern Hemisphere. *Mon. Wea. Rev.*, **105**, 762–770, doi:10.1175/1520-0493(1977)105<0762:IVOTWS>2.0.CO;2.

Manzini, E., and Coauthors, 2014: Northern winter climate change: Assessment of uncertainty in CMIP5 projections related to stratosphere–troposphere coupling. *J. Geophys. Res. Atmos.*, **119**, 7979–7998, doi:10.1002/2013JD021403.

Martineau, P., and S.-W. Son, 2013: Planetary-scale wave activity as a source of varying tropospheric response to stratospheric sudden warming events: A case study. *J. Geophys. Res. Atmos.*, **118**, 10 994–11 006, doi:10.1002/jgrd.50871.

——, and ——, 2015: Onset of circulation anomalies during stratospheric vortex weakening events: The role of planetary-scale waves. *J. Climate*, **28**, 7347–7370, doi:10.1175/JCLI-D-14-00478.1.

McLandress, C., and T. G. Shepherd, 2009: Impact of climate change on stratospheric sudden warmings as simulated by the Canadian Middle Atmosphere Model. *J. Climate*, **22**, 5449–5463, doi:10.1175/2009JCLI3069.1.

Mitchell, D. M., S. M. Osprey, L. J. Gray, N. Butchart, S. C. Hardiman, A. J. Charlton-Perez, and P. Watson, 2012: The effect of climate change on the variability of the Northern Hemisphere stratospheric polar vortex. *J. Atmos. Sci.*, **69**, 2608–2618, doi:10.1175/JAS-D-12-021.1.

Nakagawa, K. I., and K. Yamazaki, 2006: What kind of stratospheric sudden warming propagates to the troposphere? *Geophys. Res. Lett.*, **33**, L04801, doi:10.1029/2006GL025719.

Palmeiro, F. M., D. Barriopedro, R. García-Herrera, and N. Calvo, 2015: Comparing sudden stratospheric warming definitions in reanalysis data. *J. Climate*, **28**, 6823–6840, doi:10.1175/JCLI-D-15-0004.1.

Polvani, L. M., and D. W. Waugh, 2004: Upward wave activity flux as a precursor to extreme stratospheric events and subsequent anomalous surface weather regimes. *J. Climate*, **17**, 3548–3554, doi:10.1175/1520-0442(2004)017<3548:UWAFAA>2.0.CO;2.

Quiroz, R. S., 1975: The stratospheric evolution of sudden warmings in 1969–74 determined from measured infrared radiation fields. *J. Atmos. Sci.*, **32**, 211–224, doi:10.1175/1520-0469(1975)032<0211:TSEOSW>2.0.CO;2.

Schmidt, H., and Coauthors, 2013: Response of the middle atmosphere to anthropogenic and natural forcings in the CMIP5 simulations with the Max Planck Institute Earth System Model. *J. Adv. Model. Earth Syst.*, **5**, 98–116, doi:10.1002/jame.20014.

Scott, R. K., D. G. Dritschel, L. M. Polvani, and D. W. Waugh, 2004: Enhancement of Rossby wave breaking by steep potential vorticity gradients in the winter stratosphere. *J. Atmos. Sci.*, **61**, 904–918, doi:10.1175/1520-0469(2004)061<0904:EORWBB>2.0.CO;2.

Thompson, D. W. J., and J. M. Wallace, 2000: Annular modes in the extratropical circulation. Part I: Month-to-month variability. *J. Climate*, **13**, 1000–1016, doi:10.1175/1520-0442(2000)013<1000:AMITEC>2.0.CO;2.

Uppala, S. M., and Coauthors, 2005: The ERA-40 Re-Analysis. *Quart. J. Roy. Meteor. Soc.*, **131**, 2961–3012, doi:10.1256/qj.04.176.